

## Flavonoid Oxidation by the Radical Generator AIBN: A Unified Mechanism for Quercetin Radical Scavenging

VENKAT KRISHNAMACHARI, LANFANG H. LEVINE,<sup>†</sup> AND PAUL W. PARÉ\*<sup>\*</sup>

Department of Chemistry and Biochemistry, Texas Tech University, Lubbock, Texas 79409

Four oxidized flavonoid derivatives generated from reacting quercetin (a pentahydroxylated flavone) with the peroxy radical generator 2,2'-azobis-isobutyronitrile (AIBN) were isolated by chromatographic methods and identified by NMR and MS analyses. Compounds included 2-(3,4-dihydroxybenzoyl)-2,4,6-trihydroxy-3(2*H*)-benzofuranone (**2**); 1,3,11a-trihydroxy-9-(3,5,7-trihydroxy-4*H*-1-benzopyran-4-on-2-yl)-5a-(3,4-dihydroxyphenyl)-5,6,11-hexahydro-5,6,11-trioxanaphthacene-12-one (**3**); 2-(3,4-dihydroxybenzoyloxy)-4,6-dihydroxybenzoic acid (**4**); and methyl 3,4-dihydroxyphenylglyoxylate (**5**). Product ratios under different hydrogen ion concentrations and external nucleophiles revealed that two of the products, namely the substituted benzofuranone (**2**) and the depside (**4**), are generated from a common carbocation intermediate. Indirect evidence for the operation of a cyclic concerted mechanism in the formation of the dimeric product (**3**) is provided. The identification of these products supports the model that the principal site of scavenging reactive oxygen species (ROS) in quercetin is the *o*-dihydroxyl substituent in the B-ring, as well as the C-ring olefinic linkage.

**KEYWORDS:** Quercetin; peroxy radicals; AIBN; oxidizing agents; flavonols; antioxidant

## INTRODUCTION

Flavonoids are naturally occurring polyphenolics present in fruits and vegetables and are an integral part of the human diet (1). Consumption of flavonoid-rich foods is inversely correlated with the risk of coronary heart disease, and the antioxidant or free-radical-scavenging property of flavonoids has been proposed to contribute to this chemopreventive effect (2). Radical-absorbing capacities of flavonoids have been estimated by measuring the loss of fluorescence of  $\beta$ -phycoerythrin, an indicator of oxidative damage; flavonoids compete with the fluorescent indicator to quench peroxy radical species, and reduce oxidation of  $\beta$ -phycoerythrin. On the basis of such studies, flavonoid oxygen-radical absorbing capacity increases with the number of hydroxyl substitutions in the skeleton.

Using fast reaction kinetics techniques, spectral changes for a variety of hydroxylated flavonoids and the corresponding peroxy radical species allow identification of the position of primary radical attack (i.e., formation of the peroxy radical) and the stability of the radical species formed (i.e., decay of the peroxy radical) (3). Three reactive centers have been identified by rate constant measurements as important for flavonoid radical scavenging potential: the *o*-dihydroxyl structure in the B-ring; the 2,3 double bond in conjugation with the 4-oxo function in the C-ring; and the 3- and 5-hydroxyl groups with hydrogen bonding to the keto group (for flavonoid numbering see **Figure 1**).

By chemical or enzymatic oxidation, several reaction products have been reported which provide direct evidence as to reactive site(s) of flavonoid antioxidant activity (4).

The picture emerging from these studies is that the oxidation of flavonoids is complex, resulting in a wide variety of, in many cases, unidentified reaction products. The objectives of this study were to identify products generated from the oxidation of quercetin with the peroxy radical generating agent AIBN, and to compare the levels of products formed under different reaction conditions to provide insight into the mechanism of quercetin radical scavenging.

## MATERIALS AND METHODS

**Chemicals.** Quercetin (dihydrate, 99%) was obtained from Acros Organics (Fischer Scientific; Pittsburgh, PA). AIBN (2,2'-azobis-isobutyronitrile) was purchased from Sigma-Aldrich Chemical Co (St. Louis, MO). Acetonitrile and methanol were HPLC grade and other chemicals were reagent grade.

**Oxidation with AIBN (Condition 1).** AIBN (1.97 g, 12.0 mmol, 20 equiv) was added to a solution of quercetin (200 mg, 0.6 mmol) in CH<sub>3</sub>CN (250 mL). The temperature of the reaction mixture was maintained at 60 °C for 3 h. Acetonitrile was then removed under reduced pressure, and the resulting solid was washed with hexane to remove the unreacted AIBN.

**Purification of Oxidized Products.** The quercetin oxidation reaction was run 10 times, and the pooled products were passed through a silica gel (70–230 mesh) column (55 cm × 2 cm) eluting first with CHCl<sub>3</sub> and then CHCl<sub>3</sub> with increasing concentrations of MeOH. Fractions with common TLC profiles were pooled and subsequently run through sephadex LH-20 columns (55 cm × 2 cm) eluted with MeOH. Repeated column chromatography over sephadex LH 20 yielded compounds **2** (60 mg), **3** (200 mg), **4** (52 mg), and **5** (16 mg).

\* Corresponding author. Tel: 806 742-3062. Fax: 806 742 1289. E-mail: Paul.Pare@TTU.edu.

<sup>†</sup> Current address: Dynamac Corporation, Kennedy Space Center, FL 32899.

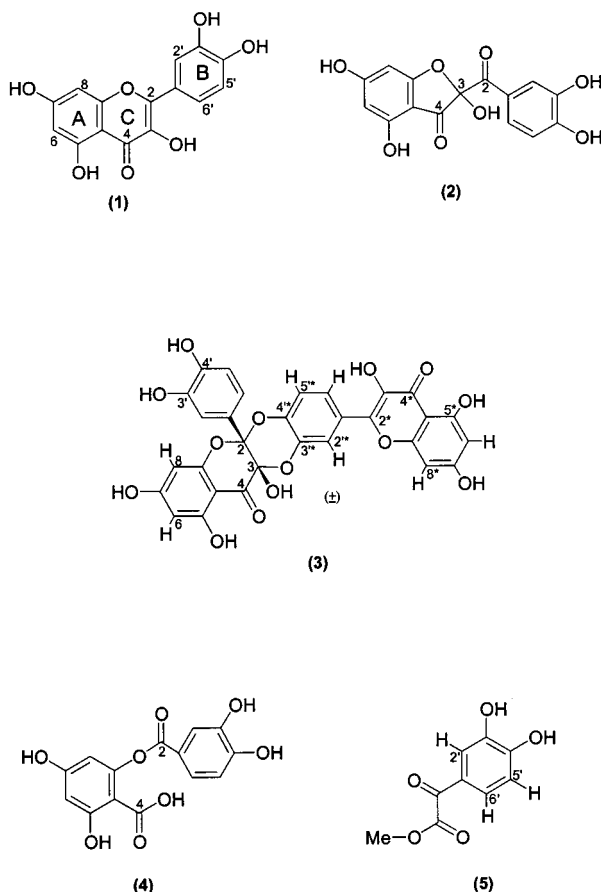


**Figure 1.** Quercetin (1) and oxidized products generated from the reaction of 1 with the radical generator AIBN.

The TLC conditions were  $\text{CHCl}_3/\text{MeOH}/\text{HOAc}$  in the ratio of 75:25:0.1 or 80:20:0.1.

**Modified Oxidation Conditions.** Quercetin (100 mg, 0.3 mmol) was dissolved in a fixed volume of 250 mL and varied ratios of acetonitrile/methanol/ethanol/concentrated HCl. To this solution AIBN (984 mg, 6.0 mmol, 20 equiv) was added, and the reaction mixture was stirred at 60 °C for 3 h. Differences in the reaction mixtures are noted as follows. For **condition 2** (low pH) 100  $\mu\text{L}$  of concentrated HCl was added to a solution of quercetin in acetonitrile (250 mL). For **condition 3** (external nucleophile) 10 mL of MeOH was added to the solution of quercetin in acetonitrile (240 mL). For **condition 4** (low pH with external nucleophile) 100  $\mu\text{L}$  of concentrated HCl was added to a solution of quercetin in acetonitrile (240 mL) and methanol (10 mL). For **condition 5** (low pH with external nucleophile) 100  $\mu\text{L}$  of concentrated HCl was added to a solution of quercetin in acetonitrile (240 mL) and ethanol (10 mL).

**Product Quantification and Data Analysis.** The oxidized products were quantified by a Hewlett-Packard 1100 series HPLC system equipped with a 250  $\times$  4.6 mm i.d., 5  $\mu\text{m}$  (Alltech) Econosphere C18 column and variable wavelength UV detector. A 2-mg aliquot of 4-hydroxybenzoic acid as an internal standard (ISTD) was added to reaction mixtures at the end of the reaction. The components of the reaction mixture (10  $\mu\text{L}$ ) were eluted with water containing 0.1%  $\text{CF}_3\text{-COOH}/\text{MeOH}$  (v/v) gradient and detected at 254 nm. The mobile phase gradient program started with 40% methanol was maintained at 40% for 15 min, increased linearly to 80% within 25 min, and kept at 80% for another 10 min. The flow rate was set to 0.5 mL/min. Analysis of variance procedure was run using SAS statistical software (5). Means were separated using Tukey's mean separation method at a *P* value less than 0.05.

**Methylation of Dimer (3).** To a solution of dimer (3) (50 mg, 83  $\mu\text{mol}$ ) in methanol, an excess of diazomethane (ca. 16 mmol) in ether was added, and the reaction mixture was allowed to stir overnight. The crude reaction mixture was then fractionated using NaOH into neutral

and acidic fractions. Preparative TLC of the neutral fraction yielded the heptamethyl derivative.

**Methylation of Depside (4).** To a solution of 4 (25 mg, 82  $\mu\text{mol}$ ) in acetone,  $\text{K}_2\text{CO}_3$  (46 mg, 4 equiv) and dimethyl sulfate (5 equiv, 38  $\mu\text{L}$ ) were added, and the resulting mixture was refluxed for 8 h. The crude pentamethyl derivative obtained was purified by Sephadex LH-20 (40 cm  $\times$  2 cm) eluted with methanol.

**$^1\text{H}$  and  $^{13}\text{C}$  NMR Spectroscopy.**  $^1\text{H}$ ,  $^{13}\text{C}$ , and 2D  $^1\text{H}$ - $^{13}\text{C}$  correlated NMR spectra were obtained in  $\text{DMSO-}d_6/\text{CD}_3\text{CN}/\text{CD}_3\text{OD}$  using a Bruker DRX 500 MHz instrument, operating at 500 MHz ( $^1\text{H}$ ) and 125 MHz ( $^{13}\text{C}$ ).

**LC-MS.** Analyses were performed on a Thermo Separation Products HPLC system coupled with a photodiode array (PDA) detector and a Thermo Finnigan (San Jose, CA) LCQ deca mass spectrometer in sequence. A 250  $\times$  2.1 mm i.d., 5  $\mu\text{m}$  Altima C18 column (Alltech) was used for separation using the same mobile phase gradient program described in the product quantification section. Trifluoroacetic acid (0.1%) or formic acid (1%) was used as a mobile phase modifier to facilitate ionization. A flow rate of 0.2 mL/min was used and directly directed to a PDA detector, then to a quadrupole ion trap mass spectrometer via an electron spray ionization or atmospheric pressure chemical ionization (APCI) interface. The mass spectrometer was operated in a negative mode; MS/MS was performed as needed.

**Compound 2.**  $^1\text{H}$  NMR ( $\text{DMSO-}d_6$ , 500 MHz): 5.89 (d,  $J = 2$  Hz, 1H, H-6), 5.94 (d,  $J = 2$  Hz, 1H, H-8), 6.79 (d,  $J = 8$  Hz, 1H, H-5'), 7.53–7.55 (m, 2H, H-2' and H-6'), 8.62 (s, 1H, OH), 9.37 (s, 1H, OH), 9.98 (s, 1H, OH), 10.79 (s, 1H, OH), 10.85 (s, 1H, OH).

$^{13}\text{C}$  NMR ( $\text{DMSO-}d_6$ , 125 MHz): 90.34 (C-8), 96.56 (C-6), 100.47 (C-4a), 104.57 (C-3), 114.89 (C-5'), 117.33 (C-2'), 123.82 (C-6'), 124.99 (C-1'), 144.73 (C-3'), 151.36 (C-4'), 158.53 (C-8a), 168.46 (C-5), 171.86 (C-7), 189.87 (C-4), 190.24 (C-2).

**Compound 2b** (water adduct).  $^1\text{H}$  NMR ( $\text{CD}_3\text{OD}$ , 500 MHz): 0.96 (t,  $J = 7$  Hz, 3H,  $\text{CH}_3$ ), 3.25–3.31 (m, 1H,  $\text{CH}_2$ ), 3.37–3.42 (m, 1H,  $\text{CH}_2$ ), 5.96 (d,  $J = 2.5$  Hz, 1H, H-6/H-8), 5.97 (d,  $J = 2.5$  Hz, H-8/H-6), 6.78 (d,  $J = 8.5$  Hz, 1H, H-5'), 7.02 (dd,  $J = 8.5$  Hz, 2.5 Hz, 1H, H-6'), 7.14 (d,  $J = 2.5$  Hz, 1H, H-2').

$^{13}\text{C}$  NMR ( $\text{CD}_3\text{OD}$ , 125 MHz): 15.31 ( $\text{CH}_3$ ), 59.92 ( $\text{CH}_2$ ), 95.08 (C-3), 97.06 (C-6/C-8), 97.44 (C-8/C-6), 101.31 (C-4a), 107.56 (C-2), 115.24 (C-5'), 117.49 (C-2'), 121.84 (C-6'), 127.05 (C-1'), 145.41 (C-3'), 147.18 (C-4'), 160.45 (C-8a), 165.16 (C-5), 168.70 (C-7), 194.14 (C-4).

**Compound 3.**  $^1\text{H}$  NMR ( $\text{DMSO-}d_6$ , 500 MHz): 2.06 (s, OH), 5.97 (bs, 2H, H-6, H-8), 6.19 (d, 1H,  $J = 2$  Hz, H-8/H-6), 6.46 (d, 1H,  $J = 2$  Hz, H-6/H-8), 6.68 (dd,  $J = 8.5$  Hz, 2.5 Hz, 1H, H-6'), 6.92 (d,  $J = 8.5$  Hz, 1H, H-5'), 7.14 (bs, 1H, H-2'), 7.26 (d,  $J = 9$  Hz, 1H, H-5'), 7.79 (d,  $J = 2$  Hz, 1H, H-2'), 7.85 (dd,  $J = 8.5$  Hz, 2 Hz, 1H, H-6'), 8.92 (s, OH), 9.16 (s, OH), 9.29 (s, OH), 9.70 (s, OH), 10.85 (s, OH), 11.14 (s, OH), 12.36 (s, OH). (Tentative assignments based on  $^1\text{H}$ - $^1\text{H}$  COSY, HMQC, HMBC, and ROESY spectra in comparison with quercetin.)

$^{13}\text{C}$  NMR ( $\text{CD}_3\text{CN}$ , 125 MHz) (tentative assignments based on  $^1\text{H}$ - $^1\text{H}$  COSY, HMQC, HMBC, and ROESY spectra in comparison with quercetin.): 91.16 (C-3), 94.82 (C-8), 97.50 (C-8\*), 98.28 (C-6\*), 99.25 (C-6), 100.88 (C-4a), 101.43 (C-2), 104.39 (C-4a\*), 115.80 (C-5'), 116.20 (C-2'), 117.60 (C-2'\*), 118.30 (C-5'\*), 121.50 (C-6'), 123.70 (C-6'\*), 126.26 (C-1'), 127.09 (C-1'\*), 137.43 (C-3), 141.46 (C-3'\*), 142.65 (C-4'\*), 144.97 (C-3'), 145.22 (C-2), 147.31 (C-4'), 157.79 (C-8a), 160.59 (C-8a\*), 162.01 (C-5), 164.73 (C-7), 165.06 (C-5), 168.90 (C-7\*), 176.51 (C-4), 188.62 (C-4\*).

**Heptamethyl Derivative of 3.**  $^1\text{H}$  NMR ( $\text{CDCl}_3$ , 500 MHz): 3.78 (bs, 3H,  $\text{OCH}_3$ ), 3.82 (s, 3H,  $\text{OCH}_3$ ), 3.85 (s, 3H,  $\text{OCH}_3$ ), 3.86 (s, 6H, 2  $\text{OCH}_3$ ), 3.87 (s, 3H,  $\text{OCH}_3$ ), 3.89 (s, 3H,  $\text{OCH}_3$ ), 6.11 (d,  $J = 2$  Hz, 1H, H-6), 6.16 (bs, 1H, H-8), 6.35 (d,  $J = 2.5$  Hz, 1H, H-6), 6.43 (d,  $J = 2.5$  Hz, 1H, H-8), 6.79 (d,  $J = 8.5$  Hz, 1H, H-5'), 7.19 (d,  $J = 8$  Hz, 1H, H-5'\*), 7.28 (dd,  $J = 8.5$  Hz, 2 Hz, 1H, H-6'), 7.35 (d,  $J = 2.5$  Hz, 1H, H-2'), 7.85–7.87 (m, 2H, H-2', H-6').

**Compound 4.**  $^{13}\text{C}$  NMR ( $\text{DMSO-}d_6$ , 125 MHz): 100.99 (C-4a), 101.73 (C-8), 104.62 (C-6), 116.19 (C-5'), 118.06 (C-2), 122.39 (C-1'), 124.39 (C-6'), 145.56 (C-3'), 151.33 (C-4'), 154.64 (C-8a), 164.15 (C-7), 166.07 (C-2), 166.11 (C-5), 172.79 (C-4). ESI-MS (negative mode): 304.9 ( $\text{M}^+ - 1$ ), 168.9 ( $\text{M}^+ - \text{C}_6\text{H}_5(\text{OH})_2\text{CO}$ ).

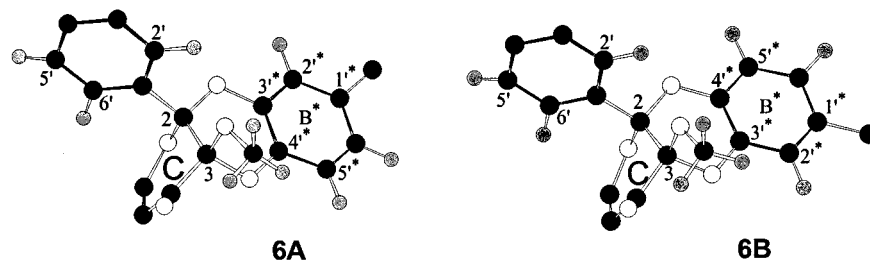


Figure 2. Partial dimer structure with dioxane linkage for the AM1 optimized regioisomers of an octamethyl dimer derivative of quercetin.

**Pentamethyl Derivative of 4.**  $^1\text{H}$  NMR ( $\text{CDCl}_3$ , 500 MHz): 3.67 (s, 3H,  $\text{COOCH}_3$ ), 3.81 (s, 3H,  $\text{OCH}_3$ ), 3.84 (s, 3H,  $\text{OCH}_3$ ), 3.93 (s, 3H,  $\text{OCH}_3$ ), 3.95 (s, 3H,  $\text{OCH}_3$ ), 6.39 (Aps, 2H, H-6, H-8), 6.92 (d,  $J = 8.5$  Hz, 1H, H-5'), 7.61 (d,  $J = 2$  Hz, 1H, H-2'), 7.79 (dd,  $J = 8.5$  Hz, 2 Hz, 1H, H-6').  $^{13}\text{C}$  NMR ( $\text{CDCl}_3$ , 125 MHz): 52.14 ( $\text{COOCH}_3$ ), 55.65 ( $\text{ArOCH}_3$ ), 56.09 (2  $\text{ArOCH}_3$ ), 56.25 ( $\text{ArOCH}_3$ ), 96.89 (C-6/8), 100.13 (C-8/6), 109.39 (C-4a), 110.39 (C-5'), 112.35 (C-2'), 121.48 (C-1'), 124.52 (C-6'), 148.78 (C-3'), 151.06 (C-8a), 153.63 (C-4'), 159.43 (C-5), 162.38 (C-7), 164.38 (C-2/C-4), 165.05 (C-4/C-2).

**Compound 5.**  $^1\text{H}$  NMR ( $\text{CD}_3\text{OD}$ , 500 MHz): 3.92 (s, 3H,  $\text{COOCH}_3$ ), 6.86 (d,  $J = 8.5$  Hz, 1H, H-5'), 7.36 (dd,  $J = 8.5$  Hz, 2 Hz, 1H, H-6'), 7.38 (d,  $J = 2$  Hz, 1H, H-2').  $^{13}\text{C}$  NMR ( $\text{CD}_3\text{OD}$ , 125 MHz): 52.96 ( $\text{COOMe}$ ), 116.28 (C-5'), 116.56 (C-2'), 125.64 (C-6'), 125.77 (C-1'), 147.11 (C-3'), 154.49 (C-4'), 166.72 ( $\text{COOMe}$ ), 186.84 (C=O). CI-MS (positive): 197 ( $\text{M}^+ + 1$ ), 137 ( $\text{M}^+ - \text{COOMe}$ ). CI-HRMS (positive): observed 197.044602;  $\text{C}_9\text{H}_9\text{O}_5$  requires 197.044999.

## RESULTS AND DISCUSSION

Quercetin (**1**) was oxidized by thermolysis of AIBN in oxygenated acetonitrile (**condition 1**). To ensure that all oxidized quercetin derivatives were produced from AIBN generated radicals, reactions devoid of AIBN or heating were also analyzed. Without the full compliment of reagents, neither the formation of products nor loss of quercetin was observed. Time-course studies carried out on the reaction revealed the presence of quercetin at the end of 1-h and 2-h intervals and its complete disappearance at the end of 3 h. The disappearance of quercetin was accompanied by the formation of a complex mixture of products, of which, at least four prominent UV absorbing products could be readily detected by TLC and HPLC. These oxidized products, isolated pure (TLC/HPLC) by column chromatography, were identified on the basis of various spectral analyses. The fused heterocyclic ring of quercetin served as the reactive center for all the oxidation products detected with an accompanying loss or gain of a substituent to the original C-ring unit (**Figure 1**).

In the least-modified of the products generated from the reaction, the pyranone C-ring of quercetin was converted to a furanone-carbonyl derivative (**2**, **Figure 1**) has been observed previously in a two-electron electrochemical (6) and a metal ion mediated oxidation (7) of quercetin. Our NMR and mass spectral data for **2** (**Figure 3**) were in agreement with the published values (6). Furthermore, our long-range C-H correlation data (HMBC) were consistent with those reported by Jungbluth et al. (7), showing that the compound formed has in fact a 3(2H)benzofuranone skeleton and not a benzopyranone skeleton.

The other major product formed from the oxidation of quercetin was **3** (**Figure 1**), a dimer that has been observed previously during the autoxidation of methyl linoleate solutions containing quercetin (8). Our spectral data are in agreement with those reported by Hirose et al. (8). However, because the oxidative coupling of two quercetin units (the *o*-dihydroxyl group of the B-ring of one quercetin unit and the conjugated

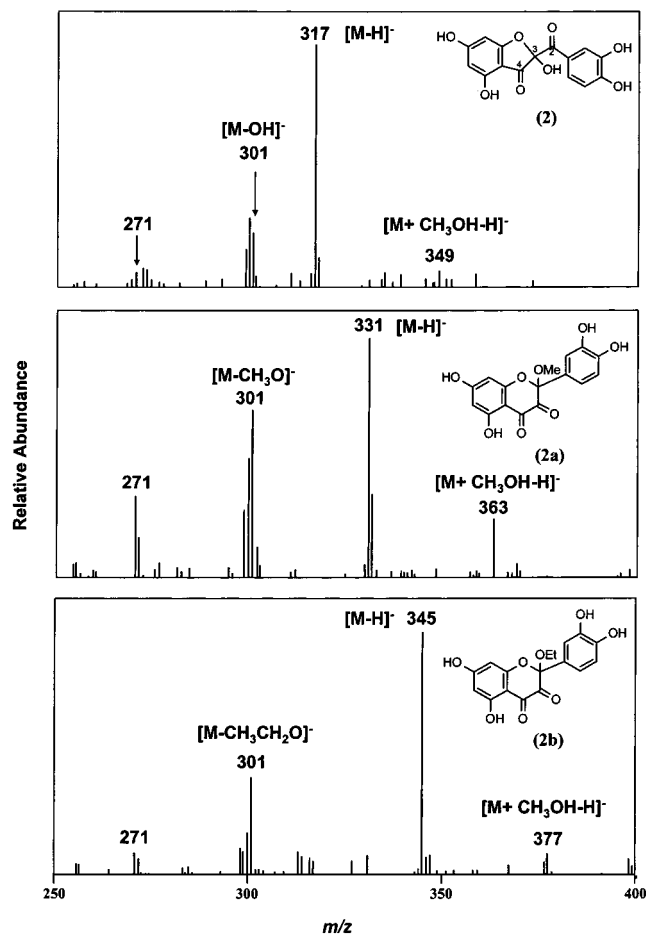


Figure 3. Atmospheric pressure chemical ionization mass spectra of the substituted 3(2H)benzofuranone (**2**), and the methoxylated (**2a**) and ethoxylated adducts (**2b**).

olefinic linkage (C-2, C-3) of the C-ring of the other) potentially gives rise to two regioisomers with either a C2-C3'/C3-C4'\* or a C2-C4'/C3-C3'\* dioxane linkage (see **Figure 2** for the dioxane linkage), we confirmed the structure by a series of NOE experiments. As the two quercetin subunits present in **3** are bridged through insulating oxygen atoms, the nature of this linkage could not be directly assigned. The absence of protons associated with the linking carbons of the two subunits also precluded any long-range carbon-proton NMR analyses of **3**. The difficulty in assigning all of the hydroxyl groups in **3** also made ROESY studies unfeasible. The structure of **3** was earlier assigned on the basis of a differential NOE observed for its methylated derivative (**8**). However, uncertainty in the spatial orientation of the B/B\* ring protons relative to the tertiary methoxyl at C-3 ruled out a definitive interpretation of the NOE interactions. To circumvent the uncertainty we carried out AM1 calculations (9), using Gaussian 94 (10) on theoretical regioisomeric octamethyl derivatives of **3** (shown as **6A** and **6B** in

**Figure 2).** AM1 is the most successful semiempirical model for predicting molecular geometry. This method parametrizes for a list of atoms including H, C, and O and partly reproduces intermolecular hydrogen bonds which is critical for biological molecules (11, 12). These Gaussian calculations provided optimized structures (**Figure 2**) from which the spatial distances between protons present in the two quercetin subunits were obtained. These distances, in turn, were used to unambiguously assign the NOE interactions that were observed in the ROESY spectrum of the heptamethyl derivative of **3**, prepared by methylating **3** using diazomethane. The calculations revealed that for the tertiary methoxyl group at C-3 in **6A**, the spatially closest B\* ring proton was H-2'\* at 4.5 Å (the spatial distance for H-5'\* being 6.5 Å), whereas in **6B**, H-5'\* (the B\* ring proton) was found to be the closest to the tertiary methoxyl group at 4.6 Å; H-2'\* was 6.6 Å away from the tertiary methoxyl group. These calculated distances, in conjunction with the cross-peak observed in the ROESY spectrum of the heptamethyl derivative of **3** between the C-3 methoxyl group and H-2'\*, indicated the presence of a C2–C4'\*/C3–C3'\* regioisomer and in turn confirmed the nature of the dioxane linkage in **3**. Furthermore, the cross-peak observed in the ROESY spectrum of the heptamethyl derivative, between the protons of the C-3 methoxyl and H2'/H6' of the same quercetin subunit, also established the presence of an R,R and S,S pair of stereoisomers. On the basis of the molecular modeling studies and spectral data, the dimer (**3**) was assigned the stereochemistry as shown (**3**, **Figure 1**).

The first indication of a cleaved C-ring structure for **4** (**Figure 1**), generated from the oxidation of quercetin (**condition 1**), was the absence of signals corresponding to the C2 and C3 carbons in the <sup>13</sup>C NMR spectrum. The methylation of **4** with dimethyl sulfate generated a pentamethoxy derivative with the <sup>1</sup>H NMR chemical shifts of the methyl groups indicating the presence of four phenolic hydroxyls and a carboxylic acid. The mass spectral data for **4** and its methoxyl derivative were consistent and confirmed the structural assignments. This phenolic carboxylic acid ester, a depside, has been reported under different oxidation conditions such as singlet oxygen and superoxide anion radical (13, 14), as well as in the enzyme system using quercetinase (15). However, the absence of <sup>13</sup>C NMR data in the earlier reports has raised doubts as to its correct identification (6).

The <sup>1</sup>H NMR spectrum of **5**, the fourth product of quercetin oxidation (**condition 1**), showed the absence of signals corresponding to the A-ring protons and the presence of the methyl signal of a carbomethoxyl functionality. This evidence combined with the appearance of two carbonyl functionalities in the <sup>13</sup>C NMR spectrum indicated the presence of an  $\alpha$ -keto ester moiety. The molecular ion peak, [M + H]<sup>+</sup>, at *m/z* 197 in the CI-MS (positive mode) confirmed the structural assignment. The *o*-dihydroxy benzoyl unit of this quercetin fragment presumably corresponds to the B-ring of the parent flavanoid quercetin. Product **5** to the best of our knowledge has not been observed earlier, under this or other reported oxidizing conditions. This may, at least in part, be due to its low abundance and close association with other polar reaction products.

To elucidate the reaction mechanism for quercetin radical scavenging, the abundance of the major oxidized products **2**, **3**, and **4** formed under different hydrogen ion concentration and external nucleophile were measured (**Table 1**). The values in the table represent peak HPLC areas for compounds **2**, **2a** (methoxylated adduct), **3**, and **4** under **conditions 1–4**. When ethanol was used as the external nucleophile, formation of a quercetin–ethanol adduct was observed. The formation of the

**Table 1.** HPLC Peak Areas for the Oxidized Products of Quercetin under Four Different Conditions<sup>a</sup>

product	CH <sub>3</sub> CN (condition 1)	CH <sub>3</sub> CN/H <sup>+</sup> (condition 2)	CH <sub>3</sub> CN/MeOH (condition 3)	CH <sub>3</sub> CN/MeOH/H <sup>+</sup> (condition 4)
<b>2</b>	1.83 ± 0.08 <sup>b</sup>	1.49 ± 0.09	3.40 ± 0.02	0.35 ± 0.04
<b>2a</b>	ND <sup>c</sup>	ND	ND	2.68 ± 0.25
<b>3</b>	0.95 ± 0.21	0.60 ± 0.09	3.39 ± 0.41	1.99 ± 0.42
<b>4</b>	4.86 ± 0.24	4.47 ± 0.35	3.43 ± 0.17	1.53 ± 0.13

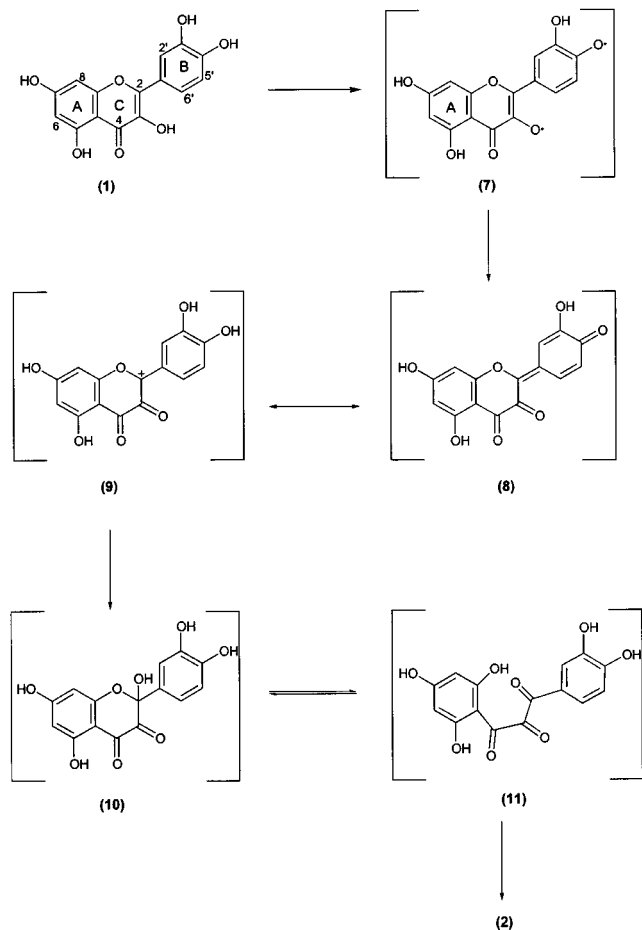
<sup>a</sup> Values ( $\times e^4$ ) represent mean peak areas from four replications. <sup>b</sup> Represents standard error. <sup>c</sup> ND, not detected.

methoxylated and the ethoxylated adducts of quercetin were observed by LC–MS (**Figure 3**) and MS–MS analyses. The quercetin–methanol adduct was not purified in sufficient quantities for NMR analyses. However, the structure of the quercetin–ethanol adduct was confirmed by a series of NMR experiments. Long-range C–H correlations observed for the carbon signal at  $\delta$ 107 with the CH<sub>2</sub> protons of the ethoxy moiety and with those of the B ring protons, established the presence of a C-2 ethoxy adduct. The signal at  $\delta$  95, for C-3, in the <sup>13</sup>C NMR spectrum of **2b** indicated the addition of water to the carbonyl at C-3. The other signals showed the expected <sup>1</sup>H and <sup>13</sup>C chemical shifts.

The level of substituted 3(2*H*)benzofuranone (**2**) and depside (**4**) decreased significantly in the presence of an external nucleophile at reduced pH (**condition 4**) compared to that of acetonitrile alone ( $p < 0.0001$ ). This decrease in accumulation of products **2** and **4** was accompanied by the appearance of the methoxylated adduct (**2a**). Interestingly there was no significant difference in dimer (**3**) formation with an external nucleophile at reduced pH or simply at a reduced pH compared to that of acetonitrile alone. It was also observed that acidification of reaction mixture (**condition 2**) did not result in any significant changes in the accumulation of products **2** and **4** ( $p < 0.0001$ ). In contrast, the addition of the external nucleophile methanol (**condition 3**) enhanced the accumulation of products **2** and **3** ( $p = 0.0003$ ), and reduced accumulation of compound **4**.

Oxidation of flavon-3-ols has been studied under several oxidizing conditions, including peroxidase oxidation (4), two-electron copper ion mediated oxidation (7, 16, 17), and DPPH/CAN treatment (18). Oxidation in nonpolar systems usually occurs via H-atom donation, and in aqueous media occurs by electron donation (19). Quercetin probably acts a chain-breaking antioxidant, which traps peroxy radicals and thus suppresses radical chain oxidation. Oxidation mechanisms are thought to vary with the oxidizing agent, and the mechanism described for a specific oxidizing agent may not directly apply to biological antioxidant systems (20). In addition, under some metal ion conditions it can be difficult to control chemical oxidation because these oxidizing agents are not specific and can react with already oxidized products. Advantages of using azo radical generators such as AIBN for probing oxidation mechanisms include the selectivity with which the radical generator yields peroxy radicals, the ability to control oxidation rates by changing temperature and/or radical generator concentrations, and the stability of the oxidized product (21). Because azo compounds decompose thermally without biotransformation they are well suited as radical sources for in vivo systems or to mimic peroxy radical reactions that occur in biological systems in vitro (22).

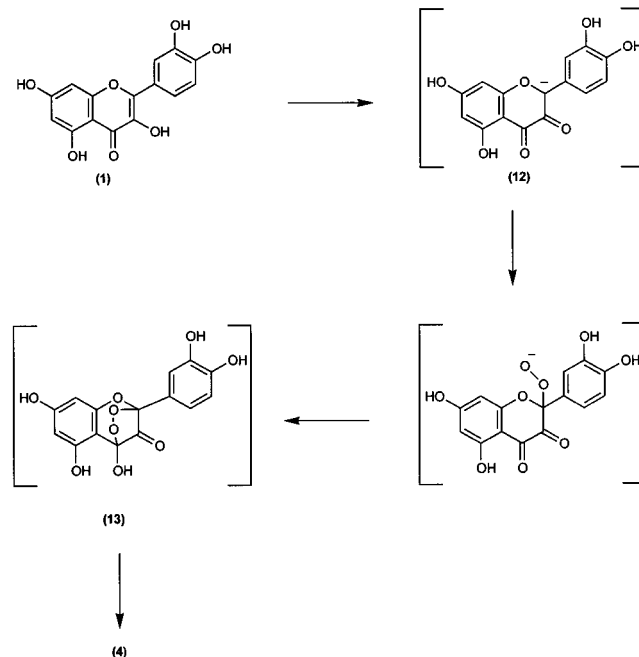
The formation of depsides and substituted 3(2*H*)benzofuranones have been reported in several oxidation systems (6, 7, 13, 14). Electrochemical oxidation of quercetin and kaempferol

**Scheme 1.** Proposed Mechanism for the Electrochemical Oxidation of Quercetin (6)

is thought to proceed through a two-electron oxidation, first to yield a 3,4-flavandione (10) which rearranges to form a substituted 3(2H)benzofuranone through the chalcone-trione ring-chain tautomer (11, **Scheme 1**) (6, 7). On the basis of reported  $pK_a$  values and the respective benzofuranone products observed, diradical (7) and quinone methide (8) (**Scheme 1**) intermediates have been proposed (6). Although the participation of a flavylium ion (9) was suspected, no further studies to substantiate the mechanism have been reported (6).

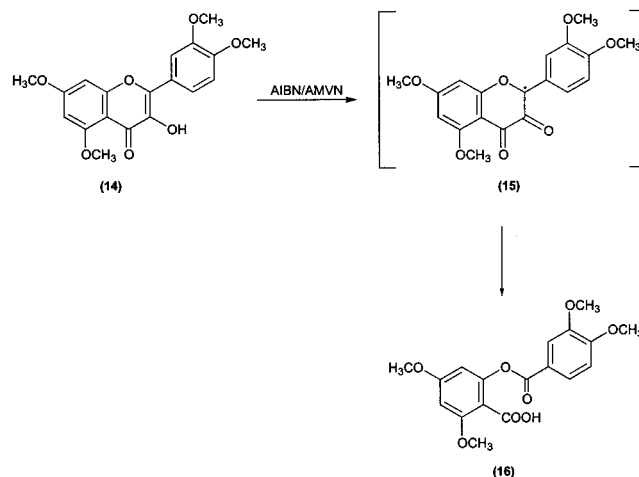
Investigations with a superoxide anion radical mediated oxidation of quercetin (**Scheme 2**) is thought to generate a C-2 centered anion (12) followed by a cyclic peroxide (13) rearranging to the depside product (13, 14). Using AMVN and AIBN as radical initiators and tetramethylquercetin (14) as substrate, the depside observed (16) has been proposed to be generated via a C-2 centered radical (15, **Scheme 3**). However, direct evidence for this mechanism was not provided (23, 24).

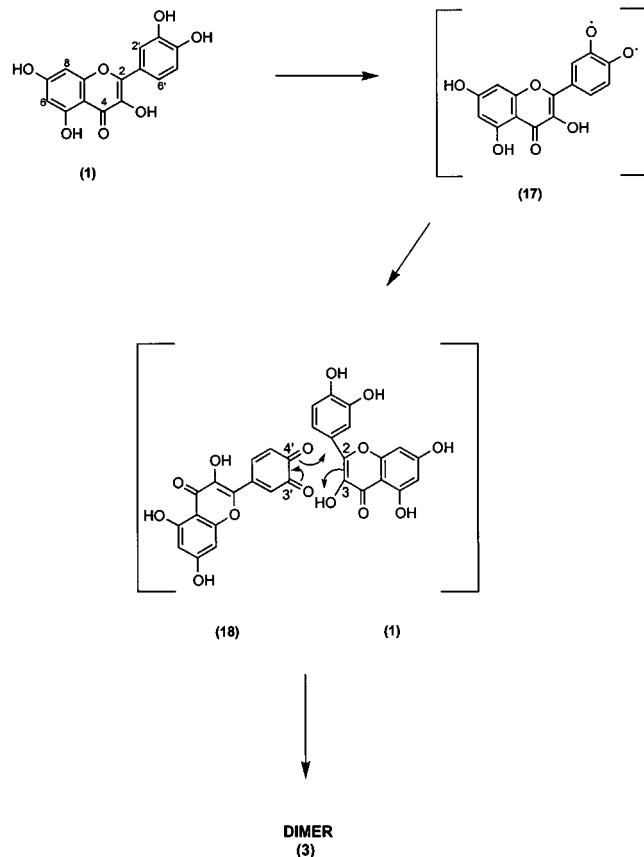
Our studies do not support such an anion radical mechanism for the formation of either 2-(3,4-dihydroxybenzoyl)-2,4,6-trihydroxy-3(2H)benzofuranone (2) or the depside (4). By varying the acidity and available nucleophile we provide evidence for a common carbocation intermediate, (9, **Scheme 1**), while such an intermediate is not involved in the formation of the dimer (3). The strong electrophilic nature of the intermediate (9) is evident from the methoxylated and ethoxylated adducts (2a, 2b, **Figure 3**) observed with the addition of methanol and ethanol to the reaction mixture (conditions 4 and 5), respectively (see **Figure 3** for MS profile). Statistical analyses of the peak areas for several of the products obtained

**Scheme 2.** Proposed Mechanism for Superoxide Anion Radical Mediated Oxidation of Quercetin (13, 14)

from four replications (**Table 1**) revealed that the levels of 2 and 4 under **condition 4** are significantly lower than the corresponding levels formed under **conditions 1–3**. The increase in hydrogen ion concentration in the reaction medium promotes the formation and stabilization of the cation intermediate (9) and thus facilitates the attack by an external nucleophile. It appears that methanol or ethanol competes with water and the peroxides present in the medium for the attack on 9. The increase in the level of the methoxylated adduct with the concomitant decrease in the levels of 2 and 4 under **condition 4** (**Table 1**), points to such competitive reactions occurring in the medium and thus the presence of the carbocation intermediate 9. The fact that the increase in hydrogen ion concentration in the reaction mixture does not significantly alter amounts of 2, 3, and 4 in **condition 2** shows that this shift in pH does not prevent or interfere with the initiation and propagation of free radical processes occurring in the reaction medium.

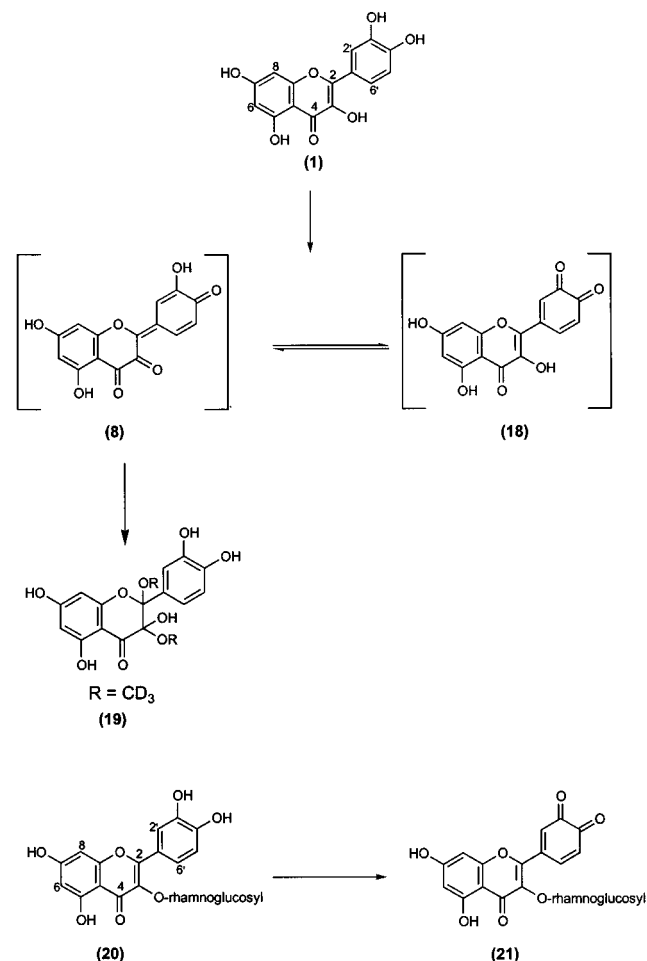
These observations are consistent with the existence of a C-2 centered carbocation intermediate (9, **Scheme 1**) in the formation

**Scheme 3.** Proposed Mechanism for AIBN/AMVN Mediated Oxidation of Tetramethylquercetin (23, 24)

**Scheme 4.** Proposed Mechanism for Formation of the Quercetin Dimer (3), Mediated by AIBN

of 2 and 4. The diradical (7, **Scheme 1**) formed by two successive one electron oxidations gives rise to a *p*-quinone methide species (8, **Scheme 1**) which is in equilibrium with the flavylium ion and thus with the C-2 centered carbocation species 9.

Product 3, the doubly linked dimer, represents the active involvement of B-ring in the radical scavenging properties of quercetin. The formation of a syn pair (RR and SS) of diastereoisomers of 3 points to a concerted Diels–Alder type mechanism. The involvement of a carbocation intermediate such as 9 (**Scheme 1**) in the formation of the doubly linked dimer 3 is ruled out because dimer formation was unaffected by the availability of an external nucleophile at reduced pH (**condition 4**). The operation of a radical coupling mechanism for the formation of 3 also appears unlikely based on the lack of dimer observed when kaempferol is substituted for quercetin. Kaempferol, which possesses a reactive hydroxyl at C-4' but not the 3' OH, would be expected to give rise to a dimer under a radical mechanism while being incapable of doing so via a concerted reaction (unpublished observation). Thus, the formation of 3 from quercetin likely goes through a concerted reaction between the B-ring *o*-quinone moiety (18, **Scheme 4**) and the C-2/C-3 double bond of ring C of another quercetin unit (**Scheme 4**). The high regioselectivity (C-2/C-4'\*<sub>2</sub>, C-3/C-3'\*<sub>2</sub> linkage) observed cannot be unambiguously explained by such a concerted mechanism. In addition, the role of the C-3 hydroxyl in the formation of 3 is unclear, although its presence is essential in the formation of the dimer. Indeed, luteolin, a deoxy analogue of quercetin, which lacks a C-3 hydroxyl group, fails to generate any dimeric products on oxidation with AIBN (**condition 1**; unpublished observation).

**Scheme 5.** Proposed Mechanism for DPPH/CAN Mediated Oxidation of Quercetin and Rutin (18)

It is interesting to note that the external nucleophile methanol (**condition 3**) triggers an increase in the accumulation of the products 2 and 3, accompanied by a decrease in 4. A possible explanation for this increase in product formation is that methanol, under **condition 3**, promotes the radical-hydrogen atom abstraction process, thereby increasing the amount of the diradical intermediates 7 (**Scheme 1**) and 17 (**Scheme 4**). The disproportionate accumulation of the substituted 3(2*H*)benzofuranone product [2] relative to the depside [4] may be due to a higher level of water relative to that of peroxide.

The presence of a B-ring *o*-quinone intermediate has been proposed in the DPPH/CAN mediated oxidation of quercetin (**Scheme 5**) (5). On the basis of kinetic data, a methanol adduct (19, **Scheme 5**) was proposed to be formed via a tautomeric equilibrium of quercetin *o*-quinone (18, **Scheme 5**) and *p*-quinone (8, **Scheme 5**). With the O-sugar derivative of quercetin, rutin (20, **Scheme 5**), which is glycosylated at the 3-position, an *o*-quinone intermediate (21) is observed, establishing the presence of such an *o*-quinone intermediate in the oxidation of quercetin. Awad et al (4) reported a peroxidase mediated one electron oxidation of quercetin in the presence of glutathione wherein the formation of C-6/C-8 glutathionyl adducts of quercetin were observed. These adducts were explained by invoking the B-ring *o*-quinone and its *p*-quinone methide isomers providing an indirect evidence for their existence.

In the case of AIBN generated radicals reacting with quercetin, it appears that both the *ortho* and *para* quinone intermediates are formed by the successive abstraction of two

hydrogen atoms at positions 3' and 4' or 4' and 3, respectively. The dimeric product (**4**) observed from the *o*-quinone reaction, we propose, is formed via a Diels–Alder type addition, whereas the substituted 3(2*H*)benzofuranone (**2**) and depside (**4**) are generated from the *p*-quinone via a carbocation intermediate. Interestingly, an increase in AIBN in the reaction of quercetin causes a shift of products, with a significant decrease of the dimeric component and an increase of the depside and substituted 3(2*H*)benzofuranone products. This suggests the possible interconversion of the *o*-quinone and *p*-quinone intermediates, which is currently under investigation.

#### ABBREVIATIONS USED

AIBN, 2,2'-Azobisisobutyronitrile; AMVN, 2,2'-azobis-(2,4-dimethyl valeronitrile); DPPH, 1,1-diphenyl-2-picrylhydrazyl; CAN, Ceric ammonium nitrate.

#### ACKNOWLEDGMENT

We thank David Purkiss for expert NMR technical support. We thank Richard Jasoni for assistance with the statistical analysis. Constructive comments concerning an earlier version of the manuscript were provided by D. Birney and G. Li.

#### LITERATURE CITED

- Hollman, P. C. H.; van Trijp, J. M. P.; Buysman, M. N. C. P.; Gaag, M. S. V. D.; Mengelers, M. J. B.; Vries, J. H. M.; Katan, M. B. Relative bioavailability of the antioxidant flavonoid quercetin from various foods in man. *FEBS Lett.* **1997**, *418*, 152–156.
- Geleijnse, J. M.; Launer, L. J.; van der Kurp, D. A. M.; Hofman, A.; Witteman, J. C. M. Inverse association of tea and flavonoid intakes with incidence of myocardial infarction: the Rotterdam Study. *Am. J. Clin. Nutr.* **2002**, *75*, 880–886.
- Pannala, A. S.; Chan, T. S.; O'Brien, P. J.; Rice-Evans, C. A. Flavonoid B-ring chemistry and antioxidant activity: Fast reaction kinetics. *Biochem. Biophys. Res. Commun.* **2001**, *282*, 1161–1168.
- Awad, H. M.; Boersma, M. G.; Vervoort, J.; Rietjens, M. C. M. Peroxidase-catalyzed formation of quercetin quinone methide-gluthione adducts. *Arch. Biochem. Biophys.* **2000**, *378*, 224–233.
- Statistical Analysis Systems Institute Inc. SAT/STAT User's Guide, Version 6.11, Vol. 1; SAS: Cary, NC, 2001.
- Jorgensen, L. V.; Cornett, C.; Justesen, U.; Skibsted, L. H.; Dragsted, L. O. Two-electron electrochemical oxidation of quercetin and kaempferol changes only the flavonoid C-ring. *Free Radical Res. Commun.* **1998**, *29*, 339–350.
- Jungbluth, G.; Rühling, I.; Ternes, W. Oxidation of flavonols with Cu(II), Fe(II) and Fe(III) in aqueous media. *J. Chem. Soc., Perkin Trans. 2* **2000**, 1946–1952.
- Hirose, Y.; Fujita, T.; Nakayama, M. Structure of doubly-linked oxidative product of quercetin in lipid peroxidation. *Chem. Lett.* **1999**, 775–776.
- Dewar, M. J. S.; Zoebisch, E. G.; Healy, E. F.; Stewart, J. J. P. The development and use of quantum-mechanical molecular models. 76. AM1 - A new general-purpose quantum-mechanical molecular model. *J. Am. Chem. Soc.* **1985**, *107*, 3902–3909.

- Frisch, M. J.; Trucks, G. W.; Schlegel, H. B.; Gill, P. M. W.; Johnson, G. G.; Robb, M. A.; Cheeseman, J. R.; Keith, T.; Petersson, G. A.; Montgomery, J. A.; Raghavachari, K.; Al-Laham, M. A.; Zakrzewski, V. G.; Ortiz, J. V.; Foresman, J. B.; Cioslowski, J.; Stefanov, B. B.; Nanayakkara, A.; Challacombe, M.; Peng, C. Y.; Ayala, P. Y.; Chen, W.; Wong, M. W.; Andres, J. L.; Replogle, E. S.; Gomperts, R.; Martin, R. L.; Fox, D. J.; Binkley, J. S.; Defrees, D. J.; Baker, J.; Stewart, J. P.; Head-Gordon, M.; Gonzalez, C.; Pople, J. A. *Gaussian 94*, revision E.2; Gaussian Inc.: Pittsburgh, PA, 1995.
- Zerner, M. Semiempirical Molecular Orbital Method. In *Reviews in Computational Chemistry II*; Lipkowitz, K. B., Boyd, D. B., Eds.; VCH: New York, 1991.
- Levine, I. N. *Quantum Chemistry*. Prentice Hall: Upper Saddle River, NJ, 2000; pp 582–583.
- Kano, K.; Mabuchi, T.; Uno, B.; Esaka, Y.; Tanaka, T.; Iinuma, M.; Superoxide anion radical-induced dioxygenolysis of quercetin as a mimic of quercetinase. *J. Chem. Soc., Chem. Commun.* **1994**, 593–594.
- Tournaire, C.; Hocquaux, M.; Beck, I.; Oliveros, E.; Maurette, M. Activité anti-oxidante de flavonoïdes Réactivité avec le superoxyde de potassium en phase hétérogène. *Tetrahedron* **1994**, *50*, 9303–9314.
- Brown, S. B.; Rajananda, V.; Holroyd, A.; Evans, E. G. V. A study of the mechanism of quercetin oxygenation by <sup>18</sup>O labeling. *Biochem. J.* **1982**, *205*, 239–244.
- Utaka, M.; Takeda, A. Copper(II)-catalyzed oxidation of quercetin and 3-hydroxyflavone. *J. Chem. Soc. Chem. Commun.* **1985**, 1824–1826.
- Balogh-Hergovich, E.; Speier, G. Oxidation of 3-hydroxyflavones in the presence of copper(I) and copper(II) chlorides. *J. Mol. Catal.* **1992**, *71*, 1–5.
- Dangles, O.; Fargeix, G.; Dufour, C. One-electron oxidation of quercetin derivatives in protic and non protic media. *J. Chem. Soc., Perkin Trans. 2* **1999**, 1387–1395.
- Jovanovic, S. V.; Steenken, S.; Hara, Y.; Simic, M. G. Reduction potentials of flavonoid and model phenoxyl radicals. *J. Chem. Soc., Perkin Trans. 2* **1996**, 2497–2504.
- Awad, H. M.; Boersma, M. G.; Vervoort, J.; Rietjens, M. C. M. Peroxidase-catalyzed formation of quercetin quinone methide-gluthione adducts. *Arch. Biochem. Biophys.* **2000**, *378*, 224–233.
- Arora, A.; Valcic, S.; Lorenzo, S.; Nair, M. G.; Timmermann, B. N.; Liebler, D. C. Reactions of Genistein with Alkyl peroxy Radicals. *Chem. Res. Toxicol.* **2000**, *13*, 638–645.
- Niki, E. Free radical initiators as source of water or lipid soluble peroxy radicals. *Methods Enzymol.* **1990**, *186*, 100–108.
- Ohashi, H.; Kyogoku, T.; Ishikawa, T.; Kawase, S.; Kawai, S. Antioxidative activity of tree phenolic constituents 1: Radical-capturing reaction of flavon-3-ols with radical initiator. *J. Wood Sci.* **1999**, *45*, 53–63.
- Ishikawa, T.; Takagi, M.; Kanou, M.; Kawai, S.; Ohashi, H. Radical-capturing reaction of 5,7,3',4'-tetramethylquercetin with the AIBN radical initiator. *Biosci., Biotechnol., Biochem.* **1999**, *63*, 173–177.

Received for review January 14, 2002. Revised manuscript received May 8, 2002. Accepted May 8, 2002. This research was supported by the Robert Welch Foundation (grant D-1478).

JF020045E